The Size of the Unstirred Layer as a Function of the Solute Diffusion Coefficient

Peter Pohl, Sapar M. Saparov, and Yuri N. Antonenko
Medizinische Fakultät, Institut für Medizinische Physik und Biophysik, Martin-Luther-Universität, 06097 Halle, Germany

ABSTRACT By monitoring the concentration distribution of several solutes that are diffusing at the same time under given mixing conditions, it was established that the unstirred layer (USL) has no clearly defined boundary. For the cases of solute permeation and water movement across planar bilayer lipid membranes, respectively, experiments carried out with double-barreled microelectrodes have shown that the thickness of the USL depends on which species is diffusing. Small molecules with a larger diffusion coefficient encounter an apparently thicker USL than larger molecules with a smaller diffusion coefficient. The ratio of the USL thicknesses of two different substances is equal to the third root of the ratio of the respective diffusion coefficients. This experimental finding is in good agreement with theoretical predictions from the theory of physicochemical hydrodynamics.

INTRODUCTION

Adjacent to a membrane there is usually a stagnant layer that acts as an additional diffusion barrier so that rapidly permeating substances could actually be rate-limited by diffusion (Barry and Diamond, 1984). Osmotic volume flow across membranes is also affected by unstirred layers (USL), because the movement of the solvent will carry dissolved solutes along with it (Schafer and Andreoli, 1987). That, in turn, may alter the osmotic gradient across the membrane (Fettiplace and Haydon, 1980). Concentration gradients of the solute induced within the USL both in the cases of solute permeation and osmosis play an essential role in the transport process across biological membranes (Läuger, 1976; Finkelstein, 1987). Their size and importance depend on the rate of dissipation through back diffusion of the solute and on the various stirring effects that may be present (Pedley, 1983).

For example, the importance of USLs has been demonstrated in models of intestinal adaptation where nutrient uptake is enhanced by alterations in the passive permeability properties of the intestinal brush border membrane (Thomson et al., 1996). In the vicinity of enterocytes the USL causes a significant diffusive resistance to the uptake of hydrophobic xenobiotics (polychlorinated biphenyls) dissolved in dietary fat (Dulfer et al., 1996). The USL adjacent to the internal capillary wall is assumed to cause the blood-flow dependency in adsorption (Chiou, 1996). Also, cholesterol efflux from cell membranes is influenced by the diffusion of cholesterol molecules through the extracellular unstirred water layer (Rothblat et al., 1992). Diffusion through the unstirred layer, which may exist in Disse's space in isolated perfused livers (and probably under in vivo conditions), limits the hepatic uptake rate of protein-bound ligands (Schwab and Goresky, 1996; Ichikawa et al., 1992) and of drugs with extremely high membrane permeabilities (Miyauchi et al., 1993). The erythrocyte membrane permeability to the rapidly penetrating compound ammonia is rate-limited by diffusion through USLs at basic pH (Labotka et al., 1995). Existence of the USL slows the uptake of O_2 by red cells of man by a factor of at least 1.8–2.0 (Holland et al., 1985).

The uptake of rapidly permeating substances as well as the regulation of secretion may be governed by stagnant water layers. Increases in luminal flow rate, for example, directly increase apical membrane H^+ secretion in the proximal tubule, possibly by modification of a luminal USL (Preisig, 1992). Hemodynamic flow modulates the effects of adenine nucleotides on vascular endothelial cells by changing the nucleotide concentration at the cell surface (Shen et al., 1993).

Usually, diffusive restrictions arising from the presence of stagnant water layers are estimated from the diffusion coefficient and the USL thickness (δ):

$$P^{\delta} = D/\delta \tag{1}$$

Thereby, the problem of determining the permeability of the USL, P^{δ}, is transformed into the task of evaluating δ. Mostly, the latter is calculated from the time course for the buildup or depletion of a solute adjacent to a membrane barrier (Dainty and House, 1966; Burczynski et al., 1989; Cotton and Reuss, 1989); δ can also be determined from the tracer flux if the latter has a membrane/water partition coefficient to be so high that the flux is totally limited by the USL permeability (Holz and Finkelstein, 1970).

Commonly, the thickness of the USL is assumed to be independent from the diffusion coefficient of the solute (Levitt et al., 1984; Pohl et al., 1993b; Antonenko et al.,

Received for publication 24 February 1998 and in final form 26 May 1998.

Address reprint requests to Dr. Peter Pohl, Medical Department, Institute of Medical Physics and Biophysics, Martin Luther University, 06097 Halle, Germany. Tel.: +49-345-5571243; Fax: +49-345-5571632; E-mail: peter.pohl@medizin.uni-halle.de.

Yuri N. Antonenko's permanent address is A. N. Belozersky Institute of Physico-Chemical Biology, Moscow State University, Moscow 119899, Russia.

0006-3495/98/09/1403/07 $2.00

1993, 1997; Xiang and Anderson, 1993; Strocchi et al., 1996; Jensen et al., 1997). Once determined from experiments with an indicator, δ is used to assess diffusive restrictions of other compounds (Holz and Finkelstein, 1970; Rosenberg and Finkelstein, 1978; Orbach and Finkelstein, 1980; Barry and Diamond, 1984; Xiang and Anderson, 1994; Burczynski et al., 1995). However, the validity of this approach is questionable. The distance from the membrane from where a particle migrates by diffusion depends on the competition between diffusion and convection. The distance is shortened due to vigorous stirring or, contrarily, lengthened by an increase in the mobility of the solute.

Indeed, a detailed theoretical analysis of the interaction between stirring and osmosis reveals that the size of the USL depends on the diffusion coefficient of the solute (Pedley, 1980). The same conclusion is drawn in the case of transmembrane solute diffusion (Levich, 1962).

The goal of the present work is to find experimental evidence for these theoretical predictions. Therefore, the concentration distribution of ions in the immediate vicinity of a black lipid membrane (BLM) is measured. With the help of the microelectrode technique (Lucas et al., 1975) adapted to concentration measurements near planar bilayer membranes (Antonenko and Bulychev, 1991) the size of the unstirred layer can be determined with great accuracy (Pohl et al., 1993a; Pohl et al., 1997). Experimental evidence of the functional dependency of δ on the diffusion coefficient is presented, which is in agreement with predictions from physicochemical hydrodynamics.

THEORY

Transmembrane water flux leads to solute concentration changes in the immediate membrane vicinity, i.e., water that passes through the membrane dilutes the solution it enters and concentrates the solution it leaves (Fettiplace and Haydon, 1980). The thickness δ of the stagnant water layer responsible for the polarization effect is defined in terms of the concentration gradient at the membrane water interface (Dainty and House, 1966):

$$\frac{|C_s - C_b|}{\delta} = \left.\frac{\partial C}{\partial x}\right|_{x=0}, \tag{2}$$

where x is the distance from the membrane and C_b and C_s denote the solute concentrations in the bulk and at the interface, respectively. Within the USL ($-\delta \le x \le \delta$) the solute concentration C is an exponential function of the distance x to the membrane (Pohl et al., 1997):

$$C(x) = C_s \exp\left(\frac{-vx}{D} + \frac{ax^3}{3D}\right), \tag{3}$$

where D, v, and a are the diffusion coefficient, the linear velocity of the osmotic volume flow, and the stirring parameter, respectively. Equation 3 is based on the model of stagnant point flow (Schlichting and Gersten, 1997) where the stirring velocity u ($u = a\,x^2$) in the immediate membrane vicinity is assumed to change gradually. In the most simple one-dimensional form, the balance between convection and diffusion is

$$u\frac{\partial C}{\partial x} = D\frac{\partial C}{\partial x^2} \tag{4}$$

Here the concentration distribution is considered to be independent of time. The convective flow arrives from the direction (x axis) perpendicular to the infinite plane occupied by the bilayer lipid membrane (Pedley, 1983). There it divides into a viscous flow that must adhere to the interface and a frictionless potential flow that slides along it (Schlichting and Gersten, 1997). Although the flow parallel to the membrane affects the system by convecting away a part of the solute, the steady-state concentration is a function of the distance to the membrane only and does not depend on the space coordinate parallel to the membrane (Pedley, 1983). Although proper solutions of the equations for simultaneous convection and diffusion have only been proved to be possible for a few special geometries, experimental concentration profiles in the vicinity of a planar bilayer are well described by Eq. 3 (Pohl et al., 1997). It has been shown that the agreement between theory and experiment is not satisfactory when a discrete boundary between the stirred and unstirred regions adjacent to the membrane (Dainty and House, 1966) is postulated.

Based on the model of stagnant point flow an equivalent δ value could be defined for an experiment in which the outward advection of solute by osmotic flux is limited by the inward advection of the stirring rather than by back diffusion (Pedley, 1980):

$$\delta = 1.6\left(\frac{D}{\nu}\right)^{1/3}\left(\frac{\nu}{\alpha}\right)^{1/2}, \tag{5}$$

where ν is the kinematic viscosity and α another stirring parameter that is related to a (Pohl et al., 1997):

$$0.6165(\alpha^{3/2}/\nu^{1/2}) = a. \tag{6}$$

According to Eq. 5, the size of the USL does not depend on the velocity of the volume flow. This prediction is correct only for vigorously stirred systems (Pohl et al., 1997); δ is expected to become increasingly large for rapidly diffusing substances. An augmentation of the diffusion coefficient by one order of magnitude should double δ.

In the case of rapid solute permeation across membranes, concentration gradients are also generated within the USL. The transmembrane movement of solutes can be regarded as a heterogeneous reaction that involves several steps. The first one is the transfer of the solute to the membrane surface. In a second step the heterogeneous reaction itself takes place. Examples are the binding of the solute to a carrier (Winne, 1973), the proton uptake by protonophores (McLaughlin and Dilger, 1980) or the dissociation of weak acids and bases (Gutknecht and Tosteson, 1973), adsorption

or desorption, etc. Finally, the reaction products are transferred from the reaction site. The overall rate of the heterogeneous reaction, when governed by diffusion kinetics, is determined by the rate of removal or introduction of reactants (Levich, 1962). The solute particles are not only entrained by the moving liquid but they also diffuse along the concentration gradient. The solution of Eq. 4 for the combined processes of convection and diffusion acquire their simplest form if the surface of a rotating disk serves as the reaction site. It is assumed that the reaction rate is sufficiently high for all particles approaching the surface to react instantaneously. Another significant characteristic of the diffusion boundary layer on a disk is the fact that its thickness is not a function of the distance from the axis of rotation, but is constant over the entire disk surface. Herein, the mathematical treatment of convective diffusion is similar to the one given above for stagnant point flow. Once the boundary conditions are equal, Eq. 5 fits also the case of solute permeation across membranes (Levich, 1962). Here the angular velocity of the rotating disk serves as the stirring parameter α.

According to the theoretical works of Levich and Pedley the USL has no clearly defined boundary; δ is a function not only of the physical properties and the velocity of the solution, but also of the diffusion coefficient. This prediction is in sharp contrast with the common assumption of the invariance of the USL thickness for a given regime of liquid motion.

MATERIALS AND METHODS

Planar bilayer lipid membranes were formed by a conventional method (Mueller et al., 1963). They were spread across a circular hole (1.1 mm in diameter) in a diaphragm separating two aqueous phases of a PTFE chamber. The membrane forming solution contained 20 mg diphytanoylphosphatidyl-choline (DPhPC, Avanti Polar Lipids, Alabaster, AL) per ml *n*-decane (Merck, Darmstadt, Germany). The aqueous salt solutions (Merck, Darmstadt, Germany) were buffered with Tris (Fluka, Buchs, Switzerland) or morpholinoethanesulfonic acid (Mes, Boehringer, Mannheim, Germany). They were agitated by magnetic stirrer bars.

An osmotic gradient was induced by urea (Laborchemie Apolda, Apolda, Germany) added to one side of the membrane only. Urea was chosen as the osmolute because it has a negligible effect on bulk viscosity. With respect to Eqs. 5 and 6 it is therefore assumed that urea does not alter δ. Because its membrane permeability of 0.04 μm/s (Finkelstein, 1976) is much lower than the water permeability, urea may be treated as nonpenetrating solute that is completely reflected by the membrane (Holz and Finkelstein, 1970; Rosenberg and Finkelstein, 1978). The transmembrane urea flux is so small that a diminution of the effective osmotic gradient between the bulk solutions (3 ml each) does not occur.

Under conditions of zero net volume flow, a net ion flux was induced with a 10-fold ion gradient in the presence of A23187 or nigericin (both Calbiochem, La Jolla, CA). DMSO-stock solutions of the nonelectrogenic ionophores were given to the *cis* aqueous compartment. In both cases, a nonelectrogenic cation/proton exchange (Antonenko and Yaguzhinsky, 1988; Pohl et al., 1990) induced concentration gradients of both cations and protons in the USLs. Here, the proton flux through the membrane is equal to the total flux of hydrogen ions (j_H), hydroxyl ions (j_{OH}), and the proton-bound buffer molecules (j_{BH}) through the unstirred layers (Borisova et al., 1974):

$$j = j_H + j_{OH} + j_B = D_H \frac{\Delta H}{\delta} + D_{OH} \frac{\Delta OH}{\delta} + D_b \frac{b \cdot \Delta pH}{\delta}, \quad (7)$$

where D_H, D_{OH}, and D_b are aqueous diffusion coefficients of H^+, OH^-, and buffer, respectively; b is the buffer capacity of aqueous solutions. Under our conditions ($b \simeq 0.6$ mM, $6 < pH < 7$) Eq. 7 is simplified to

$$j = D_b \frac{b \cdot \Delta pH}{\delta_b}, \quad (8)$$

where δ_b is the individual USL thickness of the buffer. Therefore, a pH profile measured with the microelectrode reflects the diffusion of buffer molecules toward the membrane rather than the diffusion of protons.

In the immediate vicinity of the membrane concentration profiles of two different ions were monitored simultaneously. Therefore, a double-barreled microelectrode and a reference electrode were placed at the *trans* side (unless otherwise stated) of the BLM. The ion sensitivity was achieved by filling both glass barrels with ionophore cocktails (Fluka, Buchs, Switzerland) according to the procedure described by Ammann (1986). Their tips had a diameter of ~1–2 μm. Electrodes with a 90% rise time below 0.6 s were selected. Artifacts due to a very slow electrode movement are therefore unlikely. Nevertheless, possible effects of time resolution or distortion of the USL were tested by making measurements while moving the microelectrode toward and away from the bilayer. Since no hysteresis was found, it can be assumed that an electrode of appropriate time resolution was driven without any effect on the USL.

The experimental arrangement was similar to the one described previously (Antonenko et al., 1993; Pohl et al., 1993a). Voltage sampling was performed with two electrometers (Model 617, Keithley Instruments Inc., Cleveland, OH) connected via an IEEE-interface to a personal computer. The double-barreled microelectrode was moved perpendicular to the surface of the BLM by a hydraulic microdrive manipulator (Narishige, Tokyo, Japan). The touching of the membrane was indicated by a steep potential change (Antonenko and Bulychev, 1991). From the known velocity of the electrode motion (2 μm s^{-1}), the position of the microsensor relative to the membrane was determined at any instant of the experiment. The accuracy of the distance measurements was estimated to be ± 8 μm.

For the diffusion of weak acids, it has been shown that the pH distribution within the USL can be described by an uniexponential function (Pohl et al., 1993a). The same empirical relationship was found for the concentration of an impermeable solute under conditions of a transmembrane volume flow (Pohl et al., 1997):

$$C(x) = (C_s - C_b)\exp(-x/\delta) + C_b. \quad (9)$$

In contrast to the theoretical Eq. 3 that is valid only in the interval $-\delta < x < \delta$, Eq. 9 works properly for any x ($-\infty < x < \infty$). It is worth noting that not only the signs of x and δ are different for both sides of the membrane, but the value of C_s also. Rather than simply differentiate the concentration profile as required by Eq. 2, the thickness of the USL was determined using Eq. 9. Therefore, the parametric equation was fitted to the experimental data set. For the minimization of the least-square residuals the program SigmaPlot (Jandel Corporation, San Rafael, CA) was used. This approach ensures that the standard deviation is kept small and the noise caused by the high impedance of the microelectrode is averaged.

RESULTS

Under conditions of a transmembrane volume flux, concentration profiles of calcium ions were monitored simultaneously with the distribution of sodium or potassium ions in the immediate membrane vicinity. Representative concentration profiles are shown in Figs. 1 and 2. In the example

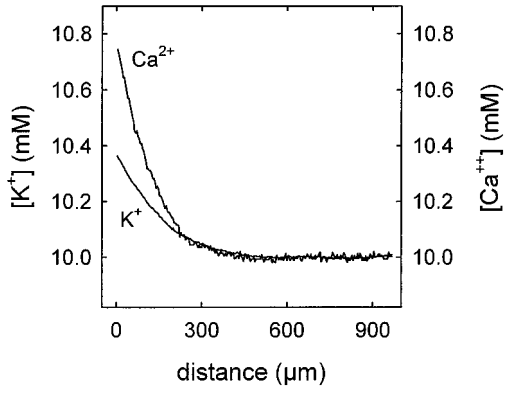

FIGURE 1 Representative calcium and potassium concentration profiles at the *trans* side of a planar membrane were monitored simultaneously by using a double-barreled microelectrode. Due to the addition of 0.8 M urea at the *cis* side a transmembrane volume flux was induced. The bulk solution contained 10 mM Tris, 10 mM Mes, 10 mM KCl, and 10 mM $CaCl_2$. From the exponential concentration profiles the thicknesses of the K^+ and Ca^{2+} USLs were derived by a curve-fitting procedure (cf. Materials and Methods, Eq. 9). They are, respectively, equal to 153 and 116 μm.

given in Fig. 1, the values for δ derived from an exponential fit (Eq. 9) were equal to 153 μm and 116 μm for K^+ and Ca^{2+}, respectively. The USL thicknesses corresponding to Na^+ and Ca^{2+} (130 μm and 105 μm, respectively) are different, too (Fig. 2). The differences in the USL thicknesses of simultaneous diffusing solutes are significant, because in subsequent series of experiments (10 runs each), δ varied by $<10\%$. Moreover, the use of a double-barreled microelectrode ensured that the concentration distributions of two different ions were measured under absolutely the same conditions. Experimental errors, for example, introduced by changes of the stirring conditions or a drift in temperature are excluded.

The experimental results are in excellent agreement with the theoretical prediction (Eq. 5). The quotient of the two

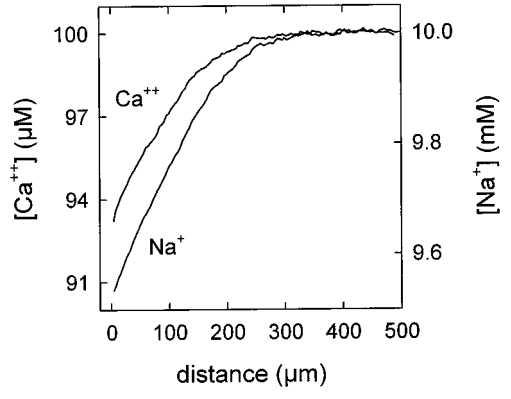

FIGURE 2 Representative calcium and sodium concentration profiles at the *cis* side of a BLM. By using a double-barreled microelectrode they were recorded simultaneously. Due to the addition of 0.3 M choline chloride at the *cis* side a transmembrane volume flux was induced. The bulk solution contained 10 mM Tris, 10 mM Mes, 10 mM NaCl, and 0.1 mM $CaCl_2$. The Na^+ and Ca^{2+} USL thicknesses were, respectively, 130 and 105 μm.

simultaneously measured δ values is related to the corresponding diffusion coefficients ($D_K = 1.96 \cdot 10^{-5}$ cm^2 s^{-1}, $D_{Na} = 1.33 \cdot 10^{-5}$ cm^2 s^{-1}, $D_{Ca} = 7.8 \cdot 10^{-6}$ cm^2 s^{-1}):

$$\frac{\delta_1}{\delta_2} = \sqrt[3]{\frac{D_1}{D_2}}. \tag{10}$$

For both cases of simultaneously measured calcium/sodium and calcium/potassium profiles Eq. 10 was satisfied (compare Fig. 5).

In a subsequent set of experiments concentration profiles were measured in the absence of an osmotic gradient. Solute transport along a calcium or potassium concentration gradient occurred after the incorporation of A23187 or nigericin into the BLM. The validity of Eq. 10 was verified for the simultaneous diffusion of calcium and Mes or Tris. The buffer diffusion coefficients ($D_{Mes} = 4.9 \cdot 10^{-6}$ cm^2 s^{-1}, $D_{Tris} = 6.6 \cdot 10^{-6}$ cm^2 s^{-1}) are taken from a previous publication (Antonenko et al., 1993). Representative cation concentration and pH profiles are shown in Fig. 3. As predicted by theory, there is no significant difference in the USL thickness of Ca^{2+} (135 μm) and Tris (139 μm). Also, the values simultaneously measured for Ca^{2+} (148 μm) and Mes (130 μm) differ only slightly (Fig. 3). Convincing evidence in favor of individual unstirred layer dimensions

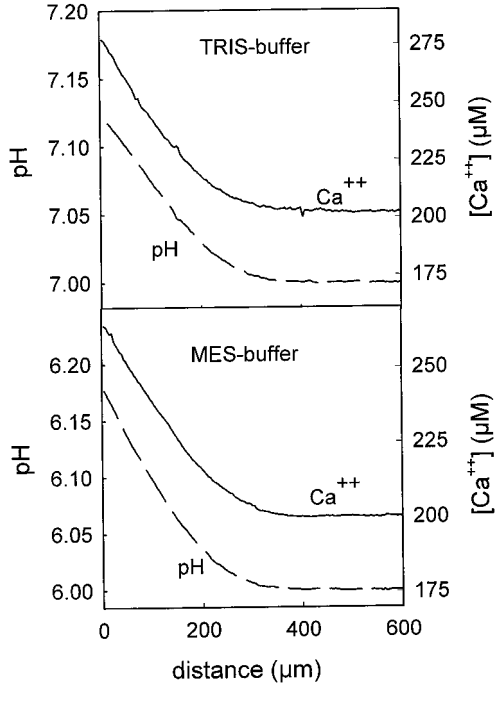

FIGURE 3 Representative cation concentration and pH profiles induced by A23187 (final concentration 5 μM) added at the *cis* side of the membrane. The double-barreled microelectrode was placed at the *trans* side of the membrane. The aqueous solutions contained 0.1 (0.1) M choline chloride and 2.0 (0.2) mM $CaCl_2$ at the *cis* (*trans*) side of the BLM. *Top:* At both sides of the membrane the solutions were buffered with 1 mM Tris. There is no significant difference in the USL thickness of Ca^{2+} (135 μm) and pH (139 μm). *Bottom:* At both sides of the membrane the solutions were buffered with 1 mM Mes. The δ values found for Ca^{2+} (148 μm) and pH (130 μm) differ only slightly.

was obtained in experiments where A23187 was substituted for nigericin. Because the diffusion of K^+ ions proceeds much faster than the diffusion of Mes, their USLs (108 and 67 μm, respectively) are very different in size (Fig. 4). In this experiment, the bulk solution at both sides of the membrane was stirred more vigorously. Therefore, the USL thicknesses are smaller than in Figs. 1–3.

All experiments are summarized in Fig. 5. With respect to different experimental conditions (first of all changes of the stirring velocity), the quotient of simultaneously measured δ is shown instead of the absolute values. For both cases of volume flow and solute transport across membranes, the USL thickness is shown to be a function of the diffusion coefficient.

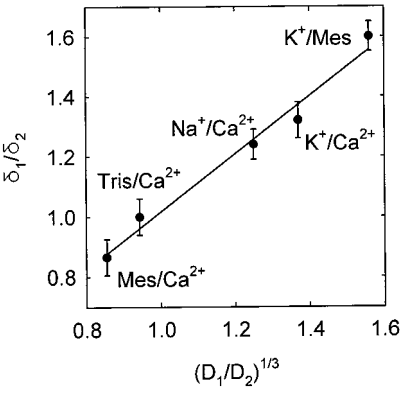

FIGURE 5 All experiments carried out under the conditions of Figs. 1–4 are summarized to show the dependence of the USL thickness on the diffusion coefficient. With respect to different experimental conditions (stirring velocity), the quotient of simultaneously measured δ is shown instead of the absolute values.

DISCUSSION

Our experiments have shown that under given experimental conditions, there is a USL thickness corresponding to each molecule diffusing in the solution. The dependence of the USL thickness on the diffusion coefficient is not taken into account by the standard physiological model of the USL. It defines, on the contrary, one unstirred water layer, where the movement of all substances takes place solely by diffusion. A priori, the standard model does not allow computation of the thickness of this layer.

Although inadequacies of the conventional USL model have been known since the approximation was introduced, it has been continued to be extensively used. Theoretical predictions based on the theory of viscous boundary layers (Schlichting and Gersten, 1997) are widely ignored, because proper solutions of the equations for simultaneous convection and diffusion have only been proved to be possible for a few special geometries (Levich, 1962; Pedley, 1980). Oversimplifying our experimental system, we have made use of models developed for stagnant point flow and the rotating disk. Despite discrepancies between the geometries in the theoretical and experimental systems that should lead to deviations in the expected distribution of the stirring velocity, the hydrodynamic approach fits well with the experimental results (Eq. 10 and Fig. 5).

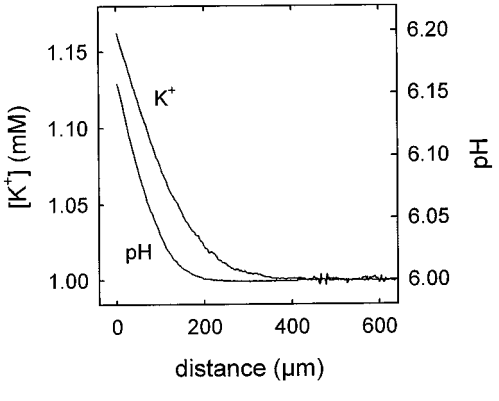

FIGURE 4 Simultaneously measured K^+ concentration and pH profiles. The aqueous solutions contained 1 (1) mM Mes, 0.1 (0.1) M choline chloride, and 1 (10) mM KCl at the *trans* (*cis*) side of the BLM. Nigericin was added to the *cis* side in a final concentration of 16 μM. The USLs found for K^+ and pH (108 and 67 μm, respectively) are very different in size.

USLs act as additional resistance ($R = \delta/D$) to solute permeation in series with the membrane resistance. To determine the true diffusional permeability of the membrane, the contribution of the USL to the observed permeability has to be considered (compare Eq. 1). Therefore, it is necessary to measure the individual δ for every solute. Commonly, however, the USL thickness is determined only for one solute that serves as a reference. For example, the permeability of planar membranes observed for water and different nonelectrolytes were corrected for USL effects with δ measured for butanol (Holz and Finkelstein, 1970; Rosenberg and Finkelstein, 1978; Orbach and Finkelstein, 1980). In these cases, the diffusion coefficients of all solutes were very close. Consequently, the differences in USL thicknesses calculated according to Eq. 10 are rather small (<20%). Because the USL correction was usually <10%, the error introduced was negligible. Only for the accurate determination of the water permeability, the USL correction was crucial because the resistance of the USL and the membrane to the water flux were comparable. In this case, the USL thickness for water was overestimated ($\delta_{water} = 0.75\ \delta_{butanol}$). Nevertheless, the error introduced is well in the range of accuracy usually indicated for tracer measurements across planar bilayers (Walter et al., 1982).

The functional dependence of the USL thickness on the diffusion coefficient given in Eq. 10 was also predicted when the reaction surface was assumed to be a smooth plate with a fluid flowing around it (Levich, 1962). This assumption is often met in physiology, i.e., in models of intestinal absorption or blood flow. For example, measurements of the absorption rates of solutes with different diffusion coefficients in intestinal loops revealed that a unique USL thickness for all substances does not exist (Levitt et al., 1988). The small molecule ($D = 2.7 \cdot 10^{-5}$ cm^2 s^{-1}), CO, encoun-

tered an apparently thicker USL than the larger warfarin ($D = 7.2 \cdot 10^{-6}$ cm^2 s^{-1}). In this case, Eq. 10 predicts that δ_{CO} is 1.34 times $\delta_{warfarin}$. Coincidentally, the measured quotient $\delta_{CO}/\delta_{warfarin}$ varied between 1.25 and 1.46 for intestinal loops with different radii (Levitt et al., 1988).

Measurements of the effective thickness of the mucosal USL in *Necturus* gallbladder epithelium provide another example (Cotton and Reuss, 1989). From the time course of the accumulation or depletion of tetramethylammonium and tetrabutylammonium at the membrane surface, a USL thickness of 50 and 42 μm, respectively, was calculated assuming an instantaneous change of the bulk concentration after addition of the substances. Again, with a value of 1.2 the ratio of the USL thickness of both substances is accurately predicted from the knowledge of the diffusion coefficients ($1.39 \cdot 10^{-5}$ and $7.6 \cdot 10^{-6}$ cm^2 s^{-1}).

Calculations of diffusion-limited kinetics for the reactions in collision coupling and receptor cross-linking have shown that diffusion is not an effective mixing mechanism; zones in which the concentration of particular molecules (e.g., enzymes, receptors) becomes depleted or enriched may form (Shea et al., 1997). Again, smaller values for D were found to correspond to a more homogeneous distribution and decreased spatial effects. Because the diffusion of proteins is much slower than the diffusion of electrolytes, their USL thicknesses are very different from each other. According to Eq. 10 K^+ encounters a two or threefold larger unstirred layer than, respectively, insulin ($D = 1.5 \cdot 10^{-6}$ cm^2 s^{-1}) or human hemoglobin ($D = 6.8 \cdot 10^{-7}$ cm^2 s^{-1}).

Measuring the USL thickness for one solute, it should be possible to predict the corresponding δ of any other solute from Eq. 10. The heterogeneity and very complex geometry of biological systems, however, may confound the analysis given above. It is possible that 1) solutes with different diffusion coefficients are equally separated from the absorptive surface and that 2) different δ values are measured for solutes having close diffusion coefficients. Studies of glucose absorption in dog small intestine provide an example for case 1. For low perfusion rates, a USL thickness of 57 μm was calculated. Because the intervillous space is only $\sim$50 μm wide (Levitt et al., 1990), more rapidly diffusing substances cannot encounter larger USLs. Similarly, highly invaginated membranes of neurons or the transverse tubular system of muscle provide unstirred regions of relatively large surface area and small volume (Barry, 1984). Case 2 is related to time course measurements, used to assess the USL thickness (Dainty and House, 1966; Dietschy et al., 1971). The time for one-half of induced concentration or potential difference change to occur is affected by membrane permeability, fluid absorption, and less than instantaneous bulk phase concentration change. Variation in these parameters unassociated with the USL can be misconstrued as alterations in δ (Lucas et al., 1992).

Obviously, the thickness of the USL depends on which species is diffusing. Experimental evidence for the simultaneous existence of several USL thicknesses has been obtained. In agreement with physicochemical hydrodynamics the size of the USL is found to be a function not only of the stirring conditions but also of the diffusion coefficient.

Financial support of the Deutsche Forschungsgemeinschaft (Germany) is grateful acknowledged (Po 533/2-1, 436 RUS 113/60).

REFERENCES

Ammann, D. 1986. Ion-Selective Microelectrodes. Principles, Design and Application. Springer-Verlag, Berlin, Heidelberg, New York, Tokyo.

Antonenko, Y. N., and A. A. Bulychev. 1991. Measurements of local pH changes near bilayer lipid membrane by means of a pH microelectrode and a protonophore-dependent membrane potential—comparison of the methods. *Biochim. Biophys. Acta*. 1070:279–282.

Antonenko, Y. N., G. A. Denisov, and P. Pohl. 1993. Weak acid transport across bilayer lipid membrane in the presence of buffers: theoretical and experimental pH profiles in the unstirred layers. *Biophys. J.* 64: 1701–1710.

Antonenko, Y. N., P. Pohl, and G. A. Denisov. 1997. Permeation of ammonia across bilayer lipid membranes studied by ammonium ion selective microelectrodes. *Biophys. J.* 72:2187–2195.

Antonenko, Y. N., and L. S. Yaguzhinsky. 1988. The ion selectivity of nonelectrogenic ionophores measured on a bilayer lipid membrane: nigericin, monensin, A23187 and lasalocid. *Biochim. Biophys. Acta*. 939:125–130.

Barry, P. H. 1984. Slow potential changes due to transport number effects in cells with unstirred membrane invaginations or dendrites. *J. Membr. Biol.* 82:221–240.

Barry, P. H., and J. M. Diamond. 1984. Effects of unstirred layers on membrane phenomena. *Physiol. Rev.* 64:763–872.

Borisova, M. P., L. N. Ermishkin, E. A. Liberman, A. Y. Silberstein, and E. M. Trofimov. 1974. Mechanism of conductivity of bimolecular lipid membranes in the presence of tetrachlortrifluormethylbenzimidazole. *J. Membr. Biol.* 18:243–261.

Burczynski, F. J., Z. S. Cai, J. B. Moran, and E. L. Forker. 1989. Palmitate uptake by cultured hepatocytes: albumin binding and stagnant layer phenomena. *Am. J. Physiol.* 257:G584–G593.

Burczynski, F. J., Z. S. Cai, J. B. Moran, T. Geisbuhler, and M. Rovetto. 1995. Palmitate uptake by cardiac myocytes and endothelial cells. *Am. J. Physiol.* 268:H1659–H1666.

Chiou, W. L. 1996. New perspectives on the theory of permeability and resistance in the study of drug transport and absorption. *J. Pharmacokinet. Biopharmacol.* 24:433–442.

Cotton, C. U., and L. Reuss. 1989. Measurement of the effective thickness of the mucosal unstirred layer in necturus gallbladder epithelium. *J. Gen. Physiol.* 93:631–647.

Dainty, J., and C. House. 1966. Unstirred layers in frog skin. *J. Physiol.* 182:66–78.

Dietschy, J. M., V. L. Sallee, and F. A. Wilson. 1971. Unstirred water layers and absorption across the intestinal mucosa. *Gastroenterology*. 61:932–934.

Dulfer, W. J., J. P. Groten, and H.-A. J. Govers. 1996. Effect of fatty acids and the aqueous diffusion barrier on the uptake and transport of polychlorinated biphenyls in Caco-2 cells. *J. Lipid Res.* 37:950–961.

Fettiplace, R., and D. A. Haydon. 1980. Water permeability of lipid membranes. *Physiol. Rev.* 60:510–550.

Finkelstein, A. 1976. Water and nonelectrolyte permeability of lipid bilayer membranes. *J. Gen. Physiol.* 68:127–135.

Finkelstein, A. 1987. Water Movement through Lipid Bilayers, Pores, and Plasma Membranes. John Wiley & Sons, New York.

Gutknecht, J., and D. C. Tosteson. 1973. Diffusion of weak acids across lipid bilayer membranes: effects of chemical reactions in the unstirred layers. *Science*. 182:1258–1261.

Holland, R.-A. B., H. Shibata, P. Scheid, and J. Piiper. 1985. Kinetics of oxygen uptake and release by red cells in stopped-flow apparatus: effects of unstirred layer. *Respir. Physiol.* 59:71–92.

Holz, R., and A. Finkelstein. 1970. The water and nonelectrolyte permeability induced in thin lipid membranes by the polyene antibiotics nystatin and amphotericin b. *J. Gen. Physiol.* 56:125–145.

Ichikawa, M., S. C. Tsao, T. H. Lin, S. Miyauchi, Y. Sawada, T. Iga, M. Hanano, and Y. Sugiyama. 1992. "Albumin-mediated transport phenomenon" observed for ligands with high membrane permeability: effect of the unstirred water layer in the Disse's space of rat liver. *J. Hepatol.* 16:38–49.

Jensen, L. J., J. N. Sorensen, E. H. Larsen, and N. J. Willumsen. 1997. Proton pump activity of mitochondria-rich cells: the interpretation of external proton concentration gradients. *J. Gen. Physiol.* 109:73–91.

Labotka, R. J., P. Lundberg, and P. W. Kuchel. 1995. Ammonia permeability of erythrocyte membrane studied by ^{14}N and ^{15}N saturation transfer NMR spectroscopy. *Am. J. Physiol.* 268:C686–C699.

Läuger, P. 1976. Diffusion-limited ion flow through pores. *Biochim. Biophys. Acta.* 455:493–509.

Levich, V. G. 1962. Physicochemical Hydrodynamics. Prentice-Hall, Englewood Cliffs, NJ.

Levitt, M. D., T. Aufderheide, C. A. Fetzer, J. H. Bond, and D. G. Levitt. 1984. Use of carbon monoxide to measure luminal stirring in the rat gut. *J. Clin. Invest.* 74:2056–2064.

Levitt, M. D., J. K. Furne, A. Strocchi, B. W. Anderson, and D. G. Levitt. 1990. Physiological measurements of luminal stirring in the dog and human small bowel. *J. Clin. Invest.* 86:1540–1547.

Levitt, M. D., J. M. Kneip, and D. G. Levitt. 1988. Use of laminar flow and unstirred layer models to predict intestinal absorption in the rat. *J. Clin. Invest.* 81:1365–1369.

Lucas, M. L., W. Schneider, F. Haberich, and J. Blair. 1975. Direct measurement by pH-microelectrode of the pH microclimate in rat proximal jejunum. *Proc. R. Soc. Lond. B.* 192:39–48.

Lucas, M. L., L. Sood, M. Mcgregor, N. Sattar, A. Watt, and J. C. Taylor. 1992. The effect of auxiliary conditions on intestinal unstirred layer diffusion modelled by numerical simulation. *J. Theor. Biol.* 159: 271–286.

McLaughlin, S., and J. P. Dilger. 1980. Transport of protons across membranes by weak acids. *Physiol. Rev.* 60:825–863.

Miyauchi, S., Y. Sawada, T. Iga, M. Hanano, and Y. Sugiyama. 1993. Comparison of the hepatic uptake clearances of fifteen drugs with a wide range of membrane permeabilities in isolated rat hepatocytes and perfused rat livers. *Pharm. Res.* 10:434–440.

Mueller, P., D. O. Rudin, H. T. Tien, and W. C. Wescott. 1963. Methods for the formation of single bimolecular lipid membranes in aqueous solution. *J. Phys. Chem.* 67:534–535.

Orbach, E., and A. Finkelstein. 1980. The nonelectrolyte permeability of planar lipid bilayer membranes. *J. Gen. Physiol.* 75:427–436.

Pedley, T. J. 1980. The interaction between stirring and osmosis. I. *J. Fluid. Mech.* 101:843–861.

Pedley, T. J. 1983. Calculation of unstirred layer thickness in membrane transport experiments: a survey. *Q. Rev. Biophys.* 16:115–150.

Pohl, P., Y. N. Antonenko, and E. Rosenfeld. 1993a. Effect of ultrasound on the pH profiles in the unstirred layers near planar bilayer lipid membranes measured by microelectrodes. *Biochim. Biophys. Acta.* 1152:155–160.

Pohl, P., Y. N. Antonenko, and L. S. Yaguzhinsky. 1990. Kinetic properties of cation-proton exchange: calcimycin (A23187)-mediated Ca^{2+}/H^{+} proton exchange on the bilayer lipid membrane. *Biochim. Biophys. Acta.* 1027:295–300.

Pohl, P., E. Rosenfeld, and R. Millner. 1993b. Effects of ultrasound on the steady-state transmembrane pH gradient and the permeability of acetic acid through bilayer lipid membranes. *Biochim. Biophys. Acta.* 1145: 279–283.

Pohl, P., S. M. Saparov, and Y. N. Antonenko. 1997. The effect of a transmembrane osmotic flux on the ion concentration distribution in the immediate membrane vicinity measured by microelectrodes. *Biophys. J.* 72:1711–1718.

Preisig, P. A. 1992. Luminal flow rate regulates proximal tubule proton, bicarbonate transporters. *Am. J. Physiol.* 262:F47–F54.

Rosenberg, P. A., and A. Finkelstein. 1978. Water permeability of gramicidin A-treated lipid bilayer membranes. *J. Gen. Physiol.* 72:341–350.

Rothblat, G. H., F. H. Hahlberg, W. J. Johnson, and M. C. Phillips. 1992. Apolipoproteins, membrane cholesterol domains, and the regulation of cholesterol efflux. *J. Lipid Res.* 33:1091–1097.

Schafer, J. A., and T. E. Andreoli. 1987. Principles of water and nonelectrolyte transport across membranes. *In* Membrane Physiology. T. E. Andreoli and J. F. Hoffmann, editors. Plenum Medical Books, London. 177–190.

Schlichting, H., and K. Gersten. 1997. Grenzschicht-Theorie, 9th ed. Springer, Berlin.

Schwab, A. J., and C. A. Goresky. 1996. Hepatic uptake of protein-bound ligands: effect of an unstirred Disse space. *Am. J. Physiol.* 270: G869–G880.

Shea, L. D., G. M. Omann, and J. J. Linderman. 1997. Calculation of diffusion-limited kinetics for the reactions in collision coupling and receptor cross-linking. *Biophys. J.* 73:2949–2959.

Shen, J., M. A. J. Gimbrone, F. W. Luscinskas, and C. F. J. Dewey. 1993. Regulation of adenine nucleotide concentration at endothelium-fluid interface by viscous shear flow. *Biophys. J.* 64:1323–1330.

Strocchi, A., G. Corazza, J. Furne, C. Fine, A. Disario, G. Gasbarrini, and M. D. Levitt. 1996. Measurements of the jejunal unstirred layer in normal subjects and patients with celiac disease. *Am. J. Physiol.* 33: G487–G491.

Thomson, A.-B. R., M. Keelan, and G. E. Wild. 1996. Nutrients and intestinal adaptation. *Clin. Invest. Med.* 19:331–345.

Walter, A., D. Hastings, and J. Gutknecht. 1982. Weak acid permeability through lipid bilayer membranes. *J. Gen. Physiol.* 79:917–933.

Winne, D. 1973. Unstirred layer, source of biased Michaelis constant in membrane transport. *Biochim. Biophys. Acta.* 298:27–31.

Xiang, T. X., and B. D. Anderson. 1993. Diffusion of ionizable solutes across planar lipid bilayer membranes—boundary-layer pH gradients and the effect of buffers. *Pharm. Res.* 10:1654–1661.

Xiang, T. X., and B. D. Anderson. 1994. The relationship between permeant size and permeability in lipid bilayer membranes. *J. Membr. Biol.* 140:111–122.